Thermal request optimization in district heating networks using a clustering approach

Thermal request optimization in district heating networks using a clustering approach

Guelpa, E., Deputato, S., & Verda, V. (2018). Thermal request optimization in district heating networks using a clustering approach. *Applied energy*, *228*, 608-617.

Available online at:
https://www.sciencedirect.com/science/article/abs/pii/S0306261918309139

Thermal request optimization in district heating networks using a clustering approach

Elisa Guelpa[a], Stefania Deputato[b], Vittorio Verda[c],

[a] Energy Deparment, Politecnico di Torino, Turin, Italy, elisa.guelpa@polito.it
[b] Energy Deparment, Politecnico di Torino, Turin, Italy, stefania.deputato@polito.it
[c] Energy Deparment, Politecnico di Torino, Turin, Italy, vittorio.verda@polito.it

Abstract:

Virtual storage in district heating systems consists in modifying the thermal request profiles of some of the connected buildings with the goal of modifying the thermal load of the plants. This approach allows one shaving the thermal peak and, consequently, reducing the primary energy consumption or connecting additional buildings to the network. Another use is related with the possibility to shift the thermal production in order to increase the possibility to compete on the electricity market. Good prediction of thermal behavior of buildings is an important aspect for managing virtual storage in order to optimize the global effect while guaranteeing the same comfort levels to the end-users. This also allows one selecting the most suitable buildings that can be considered for the implementation of such approach. In this paper, an analysis of the buildings connected to a distribution network of a large district heating system is performed, on the basis of data gathered through a monitoring system installed in the various substations. These data includes temperature and mass flow rate in the user heat exchangers available each 6 minutes. The analysis allows one identifying users with peculiar behavior, creating various clusters of buildings with similar characteristics and providing an energetic overview of the various distribution networks belonging to a large network.

Keywords:

District Heating, Peak shaving, Virtual Storage, Clustering, Optimization

1. Introduction

District heating (DH) technology represents a valuable way to provide heat and hot water to buildings, through the combined exploitation of delocalized plants, renewable sources and industrial excess heat [1, 2]. Together with high efficiency plants, such as groundwater heat pumps [3,4,5], it is expected to play an increasing role for house heating especially in urban areas. Full exploitation of the capabilities of DH systems can be only obtained through optimization of the operating conditions, which requires detailed knowledge of thermodynamic quantities along the network and in the buildings. In [6], experimental data of the exchanged heat fluxes are used in order to build a thermal load predictor, as a function of the outdoor temperature and the social behaviour of the consumers. Daily average loads and environmental conditions monitored during various years in six Swedish DH systems have been used to predict the overall thermal load [7]. In [8], the hourly thermal load provided to the local distributors is monitored for a year and used to build a model for heat demand prevision in large areas. In [9], pumping pressures in a DH network are monitored and used for testing an optimizer for minimizing pumping cost.

Information about energy flows are usually available, for existing DH systems, only for short time periods or with a low frequency (e.g. one value per day), in particular when large networks are considered. However the focus on optimal DH system management and smart heat networks, is leading, in the last year, to an increasing interest in the installation of data monitoring systems.

In [10], an introductory analysis of several substation measurements is proposed. The work analyses one year of hourly heat meter from 141 substations in two district heating networks in two cities in the south-east of Sweden. The same amount of data have been used in [11] for detecting faults regarding temperature differences and quality assurance of eliminated temperature faults. In [12] an IoT software infrastructure for city district

data management and energy flow simulations is discussed. Data gathered in the user substations of two different distribution networks are used in [13,14] with the aim of shaving the thermal peak for optimizing the peak reduction effects.

Thermal peak shaving is a very important aspect for the optimal management of DH networks. Especially in Mediterranean areas, heating systems are switched off during the night and a thermal peak occurs in the morning due to the large temperature differences taking place in the substations, when the heating system is switched on. In the case night attenuation is performed, this phenomenon is reduced, but still occurs. The presence of a peak leads to a series of disadvantages such as the reduction of the cogeneration exploitation and the increase in water mass flow rate circulating in the network. The latter involves larger pumping costs and potential limitations on the number of additional buildings which can be connected to the network without new pipelines installation. The main strategies used for the thermal peak shaving are the installation of thermal storages along the network and the application of virtual storages [13,14]. Virtual storage is intended as the use of the thermal capacity of the buildings with the goal of modifying their thermal demand profiles with the aims of reducing the thermal request at the power plants. Clearly such approach presents constrains related with the thermal comfort in the buildings.

In this work, an approach for evaluating information related to the buildings linked to a DH network is proposed starting from the data gathered through a monitoring system installed in the substations; such data are used for analysing the buildings connected to a distribution network where virtual storage is applied. Mass flow rates and temperatures at both sides of the heat exchangers are the data required for the analysis. A monitoring system has been used to gather the data; in particular, they are detected each 6 minutes. Using these data it is possible to capture information about thermal coefficients (heat transfer coefficient of the building k and its thermal capacity c) of the buildings. Furthermore, a cluster analysis based on a global coefficient of the performances allows classifying buildings into classes; such information can be used to select the more suitable users for the application of the virtual storage. The final aim of the work is to apply to the selected users a virtual storage optimizer, which includes a physical network simulator, in order to shave the thermal peak request.

2. Methodology

The goal of the work is to propose methodology for significant thermal peak shaving through the analysis of the data collected at the substations. The thermal peak shaving is performed through virtual storage, i.e. the modification of the switching on time of the user heating systems. In this work, only anticipations of the switching on time are considered for not affecting the indoor temperature at the early morning. In particular, the maximum anticipation for each user is performed through an analysis of the data collected in the user substations. The methodology of the work conduced with the aim of peak shaving is depicted in Fig. 1. At first, the data collection and the data pre-processing have been performed with the aim of achieving all the data that are mandatory for the peak shaving and for the evaluation of the maximum anticipation. Such data have been used for the evaluation of the main thermodynamic characteristics of the buildings: the equivalent heat transfer coefficient and the equivalent thermal capacity of the building. These data are grouped through a cluster analysis and for each group the maximum anticipation that can be performed is selected. In the end the optimizer for the selection of the anticipation that maximize the peak shaving is run. The optimizer includes a physical simulator of the network in order to evaluate the best peak shaving of the overall distribution network. It allows to taking into account the dynamic of the network, such as the different delay of the flow that leave the various users and the transient when the water inside the network start flowing. The various phases of the work are explained in the following paragraphs as detailed in Fig. 1.

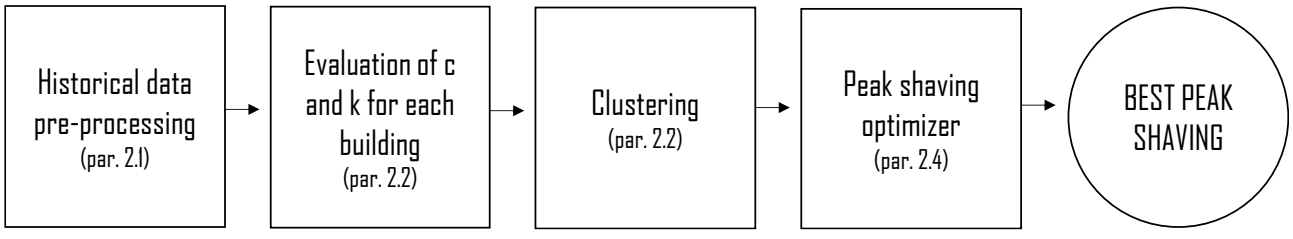

Fig. 1 Scheme of the work

2.1. Data collection system

The district heating network substations consist of an heat exchanger between the main district heating network, supplying superheated water coming from the thermal power plants (primary side), and the heating network of the building (secondary side). A simplified scheme of the substation is represented in 2. The heat exchanger on the left is the one between primary and secondary network, where the secondary network is the one bringing the hot water in the heating devices of each apartment of the building. The heat exchanger on the left is a fictitious device, which represents the heating devices (radiators, radiant floors, etc.) in the building.

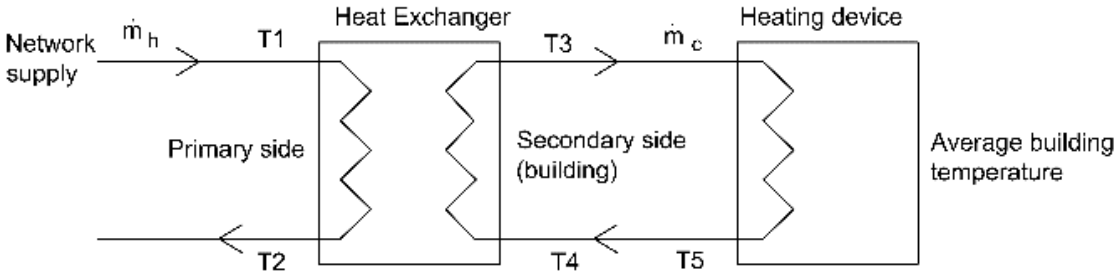

Fig. 2 Simplified scheme of the district heating network substation.

A system for monitoring the main thermodynamic quantities of the building substations has been implemented over the past years. Temperature sensors and mass flow meter are installed for collecting temperatures at the inlet and at the outlet sections of the heat exchanger and the flowing water mass flow rate. These data can be managed with the aim of achieving the heat request evolution with different external temperatures. In Figure 3 some data collected in a distribution network of the Turin DH system are shown.

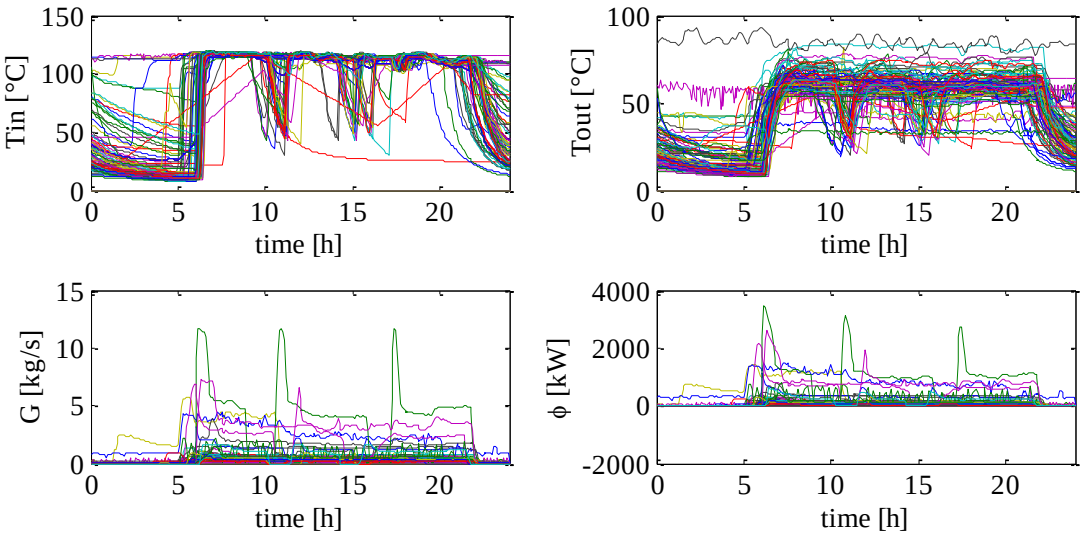

Figure 3. Data collected at the heat exchangers of some users in Turin DH system

Figure 3 depicts the evolution of the temperature at the inlet and at the outlet section at the primary side, the mass flow rate and the heat flux requested. Mass flow rate and heat power evolutions present various peaks during the day. The larger peaks occur at early morning mainly between 5 am and 8 am. The observation of the mass flow rate evolutions show that most of the heating systems are switched off during the night while only few users are never switched off. These user are also characterized by a constant temperatures at the inlet of the heating system. During the functioning of the heating systems the inlet temperature values are between

118 °C and 113 °C, due to the various distances of the users from the link between the subnetwork and the main transport network, which causes different the thermal losses values. The temperature in the outlet section depends on the inlet temperature, the mass flow rate and the heat exchanged with the secondary side. Most values for the users depicted in Fig. 3 are between 55 °C and 70 °C.

2.2. Substation and Building Model

A compact user model has been created in order to simulate the single user of the district heating network, connected to the substation. Input data of the compact user model are the primary flow and primary supply temperature together with the external one. Moreover, the characteristics of the building are needed such as: building volume, secondary flow, pipe running delay and parameters k, c.

The building model is based on a simple energy balance:

$$\phi_h - \phi_{loss} = c\,V\,\frac{d\,T_{house}}{d\,t} \tag{1}$$

The thermal losses of the building can be calculated as:

$$\phi_{loss} = k\,V\,(T_{house} - T_{est}) \tag{2}$$

The building parameters are obtained through analysis of the real data available for the building. In order to estimate the global heat transfer coefficient k, system operating conditions in the afternoon are considered. In fact, in the afternoon, typically the steady state conditions are reached (see also Fig.). In these conditions, it is possible to write:

$$\phi_h = \phi_{loss} = k\,V\,(T_{house} - T_{est}) \tag{3}$$

Performing a sensitivity analysis of the seasonal data allows one to evaluate the best value of k.
The Fig.4a shows a linear correlation between the external temperature and the thermal request in the afternoon for a sample building. Finding the fitting line it is possible to obtain values of k in the range $0.85 - 0.95\ [W/(m^3K)]$ for old buildings and $0.35 - 0.45\ [W/(m^3K)]$ or even less for new ones.

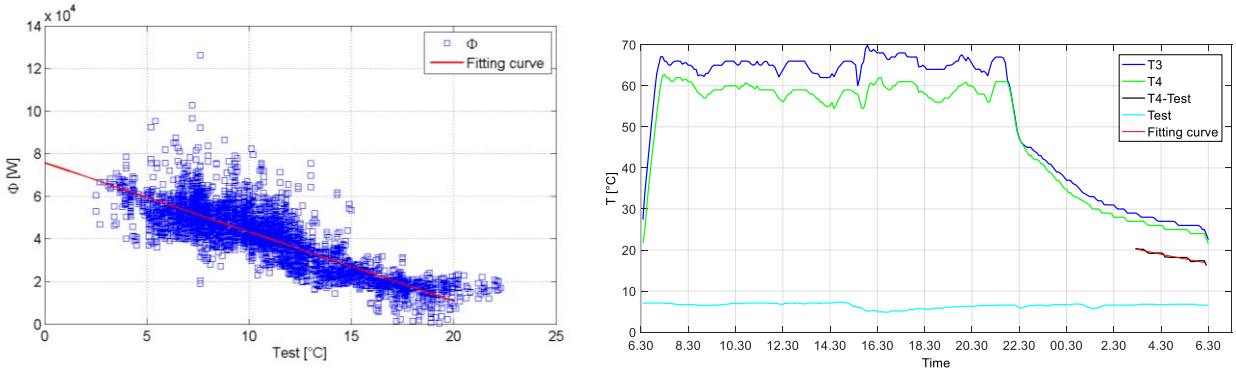

Fig. 4- K and C evaluation; a) correlation between the afternoon thermal request and the external temperature. b) *Temperatures on the secondary side of the heat exchanger in blue and green.*

Considering the transient behaviour of the building after switching off the heating system, it is possible to evaluate the thermal capacity of the building c.
In Fig. 4b are represented the temperatures T_3 and T_4 on the secondary side of the heat exchanger (blue and green curves, respectively), together with the external temperature T_{est} (light blue curve). Difference between T_4 and T_{est} in black and fitting exponential decay in red.
Black curve represents the difference $T_4 - T_{est}$ for the last hours of the transient evolution, while red curve is the theoretical exponential evolution. In the last hours of transient this exponential decay is comparable with the decay of $T_{house} - T_{est}$ since the temperature of the heating circuit becomes close to the indoor temperature. This is also highlighted by the fact that no significant difference is registered between the supply and return temperatures. The last three before the starting time are thus considered as best timeframe in order to estimate the thermal capacity of the building.
Using (1) and (2), it is possible to write:

$$k\,V\,(T_{house} - T_{est}) = -\,c\,V\,\frac{d\,T_{house}}{d\,t} \tag{4}$$

Subtracting T_{est} in the derivative and introducing $\vartheta = T_{house} - T_{est}$, one can obtain:

$$k\,\vartheta = -\,c\,\frac{d\,\vartheta}{d\,t} \tag{5}$$

The solution of (5) through integration is:

$$\vartheta = \vartheta_0\,e^{-\frac{k}{c}\cdot t} \tag{6}$$

The term $-k/c$ coincides with the power coefficient of the theoretical exponential decay represented in red in **Errore. L'origine riferimento non è stata trovata.**, therefore it is possible to obtain the value of the thermal capacity.

The thermal capacity c values are in the range $50\,000 - 150\,000\ [J/(m^3K)]$.

Referring to Fig. 2, a model of the two heat exchangers is needed in order to evaluate ϕ_h. Using the modelling approach represented in Fig.2 the environment where the fictitious device is located is characterized by an homogeneous temperature. This is thus an average building temperature, which does not necessarily coincide with the internal room temperatures, but is just representative of the internal conditions. Assuming that the current request profile is acceptable for the end-users, a different profile can be considered acceptable as well in the case the average internal conditions do not change. This particularly implies the fact that the new average temperature is never below an acceptance level achievable with the current strategy.

The difference between T_5 and T_4 is due to the pipe running delay from the outlet of the heating device to the inlet in the heat exchanger, located in the thermal power station of the building. The heat exchanger between the primary and secondary network is modelled with $\Delta T_{m\,log}$ and effectiveness-NTU method. The first calculated parameter is the design heat flux needed for the building. In the district heating network design, a typical value used to roughly design the heat exchanger is $28\ W$ for each m^3 of building volume [15].

$$\phi_D = V \cdot 28 \tag{7}$$

Once obtained the design heat flux it is possible to calculate the product $U \cdot A$ with:

$$U \cdot\ A = \frac{\phi_D}{\Delta T_{m\,log}} \tag{8}$$

where U is the global normalized heat transfer coefficient of the heat exchanger, A is the heat exchange surface and $\Delta T_{m\,log}$ is the mean logarithmic temperature difference.

Once $U \cdot A$ is calculated, it is possible to calculate the effectiveness of the heat exchanger, ε, assuming counter-flow configuration for the heat exchanger and using the corresponding effectiveness formula [16].

The heat flux is thus expressed as:

$$\phi_I = \phi_{max} \cdot\ \varepsilon \tag{9}$$

where the maximum heat exchangeable ϕ_{max} is:

$$\phi_{max} = \left(\dot{m} \cdot c_p\right)_{min} \cdot (T_1 - T_4) \tag{10}$$

These equations allow to calculate the temperatures of the two streams exiting the heat exchanger, on the basis of the inlet temperatures. The fictitious heating device has been solved in the same way, through the calculation of the effectiveness ε_h as the ratio between the heat exchanged in design conditions (assumed coincident with ϕ_D) and the maximum heat flux, namely:

$$\varepsilon_h = \frac{\phi_{h,D}}{\phi_{h,D\,max}} \tag{11}$$

$$\phi_{h,D\,max} = \left(\dot{m} \cdot c_p\right)_{min,h} \cdot (T_{3d} - T_{house,d}) \tag{12}$$

Effectiveness in off-design conditions has been considered equal to that in design conditions, which allows one evaluating the heat flux:

$$\phi_h = \phi_{h,max} \cdot\ \varepsilon \tag{13}$$

$$\phi_{h,max} = \left(\dot{m} \cdot c_p\right)_{min,h} \cdot (T_3 - T_{house}) \quad (14)$$

In this way also the second heat exchanger is solved and it is possible to calculate T_4, i.e. the return secondary temperature, which is just equal to T_5 but delayed of a certain time Δt_{delay}, characteristic of the analysed building.

The requested heat flux obtained through (13) is then used in (1) in order to evaluate the trend of the average building temperature T_{house} during the analysed day. Knowledge of the internal temperature evolution provides information about the possibilities to modify the heating system schedule. In fact, any anticipation of the switching on time leads to changes in the indoor temperature evolution, which could not be acceptable for comfort reasons and thus needs to be checked. In this work the internal temperature evolution is studied for different values of schedule modification in order to estimate the maximum acceptable anticipation for each user. A tolerance of 0.5 °C is selected and only the anticipation that leads to an indoor temperature reduction smaller than the tolerance, during the most critical time of the day, are considered.

2.3. Clustering

Once the thermal capacity and the thermal conductivity are calculated, the effects of these coefficients on the internal temperature can be evaluated with the aim of obtaining a single parameter that allows including the contribution of both terms. In particular, the indoor temperature decrease, that occurs when the heating system is switched off, has been studied for different values of k and c. The equivalent quantity U is expressed as:

$$U = \frac{k' + \mu\, d'}{1+\mu} \quad (15)$$

where

$$k' = k/\max(k) \quad (16)$$

$$d' = \frac{\frac{1}{c}}{\max\frac{1}{c}} \quad (17)$$

μ is the weight factor that allows to correlate the contribution of c and k in the decrease of indoor temperature. The value of μ is estimated through the physical model of the building expressed by equation (1), considering $\phi_h = 0$.

The quantity U is evaluated for each building considered in the analysis. The U values have been clustered into 7 groups that quantify the energetic efficiency of the buildings. Clustering is performed through a k-means approach. The aims is to associate each element x_i to one of the cluster k such that the quantity J, expressed by equation (17) is minimized.

$$J = \sum_{i=1}^{k} \sum_{i=1}^{n} \left\| x_j - R_i \right\|^2 \quad (18)$$

R is the centroid of the cluster, n is the overall number of elements and k is the number of cluster previously selected. The k-means algorithm works through an iterative technique that allows to improve the results progressively. The algorithm proceeds as reported in Fig. 5.

Once the clustering analysis has been performed, for each cluster the maximum allowed anticipation has been evaluated, through the use of the substation model.

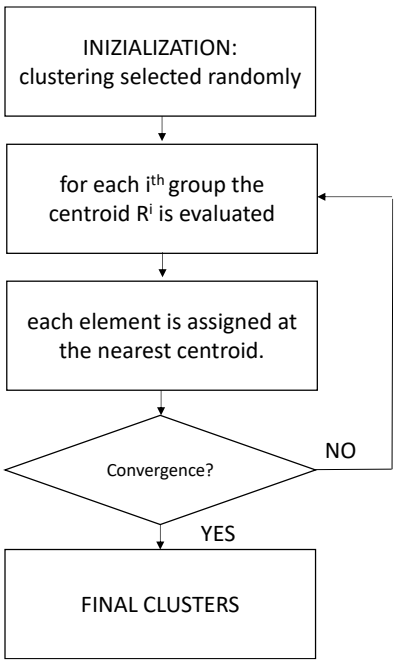

Fig. 5 k-means clustering algorithm

2.4. Virtual storage optimizer

The virtual storage optimizer aims at selecting the best set of schedule anticipations (y), i.e. the time the each heating system is switched on, that allows to maximize the peak reduction without affecting the comfort conditions for the end-users. The y variable can assume only discrete values since the time schedule allows just such discrete modifications. In particular, the time slot considered for the modifications are 10 min long. A genetic algorithm, set for integer-value, has been used to carry out the minimization.
The virtual storage optimizer has been applied to a single subnetwork of the Turin DH system. The buildings presenting high values of the energy efficiency indicator, obtained through the clustering analysis, are selected as the ones which schedule can be modified.
The objective function that has to be minimized is the maximum value of the thermal power:

$$\Phi_{\max} = \min(\Phi_{\mathrm{BCT}}(\mathrm{t})_{max}) \tag{19}$$

where $\Phi_{\mathrm{BCT}}(\mathrm{t})_{max}$ is the maximum thermal power requested by the distribution network. This is obtained considering the total mass flow rate circulating in the selected network at each time-step and the corresponding supply and the return temperatures:

$$\Phi_{\mathrm{BCT}}(\mathrm{t})_{max} = \max(\mathrm{G}_{\mathrm{TOT\_BCT}}(\mathrm{t})\ \mathrm{c_p}\ (\mathrm{T_{supply}} - \mathrm{T_{ret\_nodeBCT}}(\mathrm{t}))) \tag{20}$$

A physical network model is included in the virtual storage optimizer [17]. It is a one dimensional model based on energy conservation equations. It considers a graph approach for the network topology description [18].
The balances applied to all the nodes of the network and written in a matrix form are:

$$\mathbf{A}\cdot\mathbf{G} + \mathbf{G_{ext}} = 0 \tag{21}$$

$$\mathbf{M}\cdot\dot{\mathbf{T}} + \mathbf{K}\cdot\mathbf{T} = \mathbf{g}\,, \tag{22}$$

where G includes the mass flow rates in all the branches, Gext the mass flow rates entering and exiting the network in the nodes, M and K are the mass and the stiffness matrix, including respectively the characteristics affecting the pipeline dynamic and the coefficients of the terms depending on temperature; g includes the terms not depending on temperature. Further details on the numerical method used for the problem solving are available in [19].

The physical network model is used in order to consider the effects of the long distances involved in the network, on temperature distribution. In fact, on the return network, water exiting the substations flows and mixes with the various streams coming from the users located in the same distribution network; not all these streams are at the same temperatures because of the different distances involved. Furthermore, thermal losses affect temperature distribution, and as a result of these effects the temperature evolution at points that connects the distribution network to the transportation network is significantly different than that at the users. Therefore $T_{ret\_nodeBCT}$ has been evaluated through the thermal fluid-dynamic model

3. Results

3.1 Model Validation

One of the most important characteristic of this model is the compactness, which allows using it within an optimization logic without affecting the computational cost despite the potentially large number of buildings the model is applied to. The model has been preliminary validated through comparison with real data available for a thermal barycentre of the Turin district heating network, in Italy.

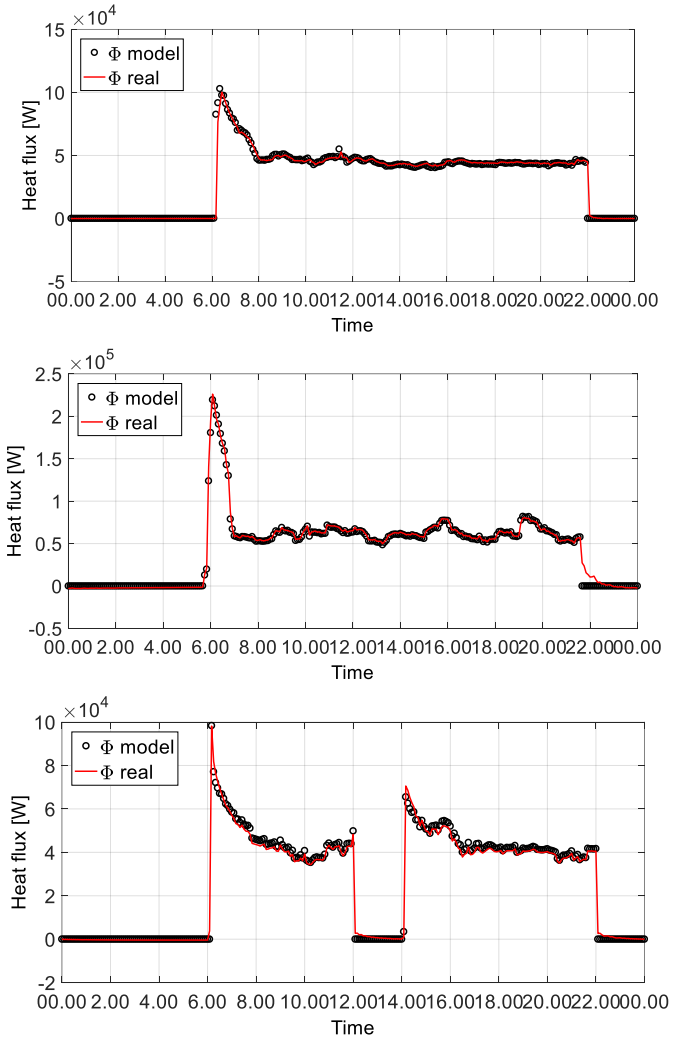

Fig. 6 In red the heat flux resulting from the model for three different users for one day of 2014. With dotted lines the experimental data in black.

In Fig. 6 the heat flux results for three example users of the Turin network are shown. Results show that the model is able to simulate the heat flux evolution with good accuracy.

3.2 Clustering Analysis

The aim of the first part of the work is to select the buildings that are more suitable for virtual storage installation. In fact, some building possess characteristics such that large anticipation are admitted while others do not. The values obtained for the thermal conductivity k and the thermal capacity c for each considered building are depicted in the scattered plot in Fig. 7.

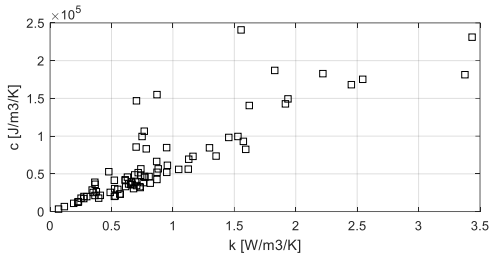

Fig. 7 k and c correlation

It is clear from Fig 7 that commonly buildings characterized by high thermal and conductivity have low heat capacity values. The global normalized coefficient U is obtained correlating the k value and the inverse of the c value through an analysis of the indoor conditions, when the heating system is switched off. In Fig. 8 the indoor temperature evolutions are reported for different k and c values. The original values are selected as the mean k and c values. Large values of k and small values of c cause fast temperature decreases. However the effects of the thermal capacity percentage variations, respect to the mean values, are larger respect to the effect obtained through the same thermal conductivity percentage variation.

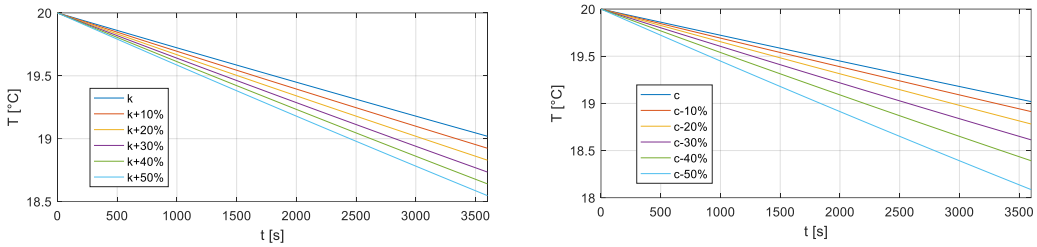

Fig. 8 Indoor temperature variation for different c and k values

In order to better visualize the influence of k and c on the indoor temperature evolution, the temperature decrease are reported in Fig. 9 for several values of k and c. Temperature variations have been evaluated considering a transient time period of an hour. This is a reasonable amount of time considering that the anticipation performed on the user are included between 0 minutes to 1 hours.

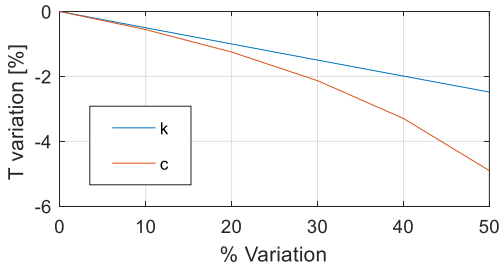

Fig. 9 Indoor temperature variation after 1 hour varying c and k

Through linearization of the results it is possible to obtain the value of μ, which allows evaluating the global normalized efficiency U for each buildings. This is 1.577.

Clustering of the buildings have been carried out using the U values; results are reported in Fig. 10. Most of the buildings analysed present low U values. This means that they have low thermal conductivity and high thermal capacity. There is only a building with U value higher than 0.5 and only 6 with values higher than 0.25. More than half of the analysed buildings are included in clusters 1 and 2.

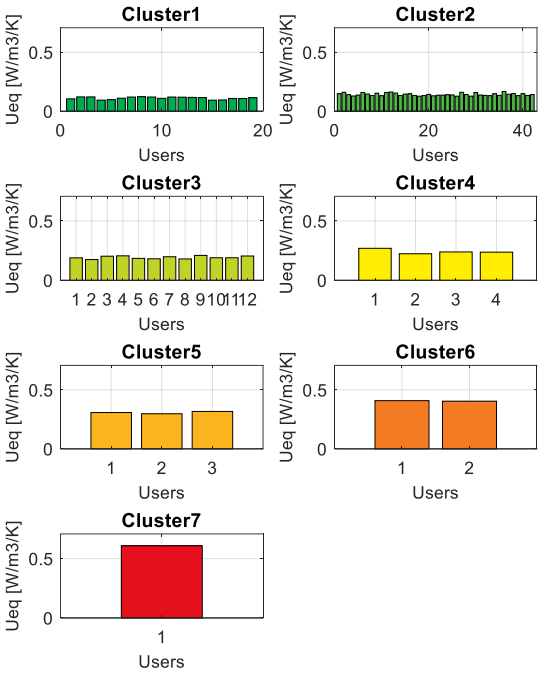

Fig. 10 Clustering results

In Fig 11, the thermal conductivity and the inverse of the thermal capacity of the buildings are depicted in a scatter plot. In addition, the cluster subdivision is also represented. As expected, the green points, that are related to the buildings with higher energetic performances, are located in the bottom left corner where thermal conductivity are low and thermal capacity high. In particular, the buildings in this area are characterized by high time constant and therefore a variation in the heating system schedule is expected not to cause quick variations in the indoor conditions. The virtual storage analysis is then applied to the buildings characterized by low values of U.

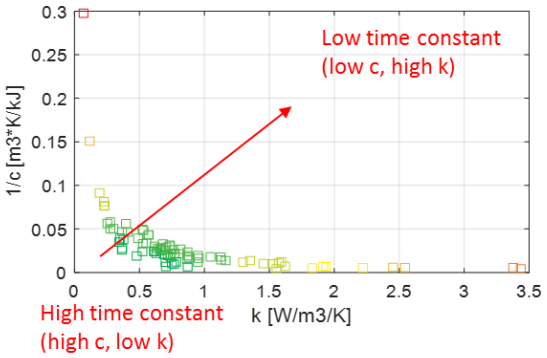

Fig. 11 Clustering represented as a function of k and 1/c

3.3 Optimization results

The virtual storage optimizer is finally applied and the set of anticipation obtained are reported in Fig. 12. The anticipation obtained are well distributed among the various possibility. The users that are not modified are 19. These are the users that have a peak that occurs in the late morning and that do not need of being anticipated. 28 users are subjected to an anticipation of 10-30 minutes. The remaining 12 users are anticipated of more than 40 minutes (40-50-60 min). These are the users whose the peak occurs in the more critical time and with a larger peak width.

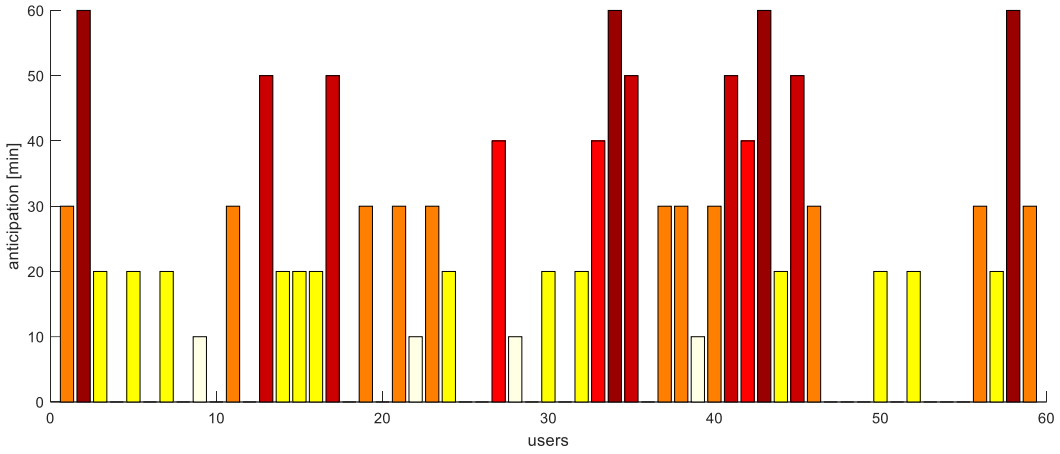

Fig. 12 Best set of anticipations

In Fig. 13, the thermal request evolutions occurring before and after the virtual storage application are reported. The dashed line is the total heat flux required to the distribution network without any modifications in scheduling; the continuous line represents the total heat flux required to the distribution network when the virtual storage is applied. It is evident from the results that the application of virtual storages yields a considerable peak reduction. The thermal request obtained with virtual storage increases before, due to the schedule anticipation. The thermal peak in the current conditions reach 11.6 MW, while the virtual storage use allows obtaining a maximum peak of about 8.5 MW. The peak reduction performed is about 25%. This is a promising result that encourage further investigations on virtual storage installation for the thermal peak shaving.

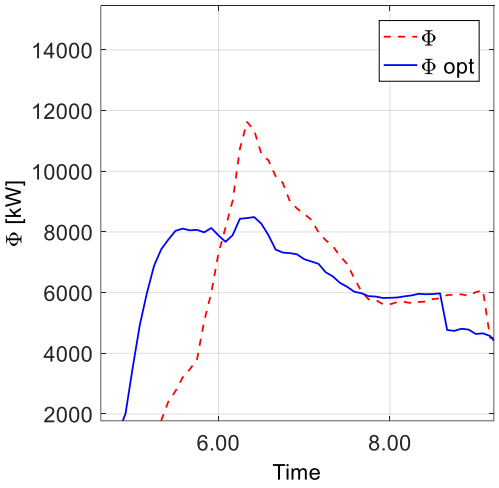

Fig. 13 Thermal peak shaving

4. Conclusions

In this work, data gathered through a monitoring system installed in the DH substation are used to estimate parameters that describe the thermal behaviour of connected buildings. These pieces of information are then used in order to identify the buildings which are more suitable for the application of virtual storage. Virtual storage optimization is then conducted with the aim of minimizing the maximum thermal request. The virtual storage optimizer includes a physical model of the network able to simulate the temperature evolution of the water that flows into the pipelines.

The analysis of the variation of the indoor temperature with different thermal conductivities and thermal capacities shows that both the variables largely affect the indoor temperature variation. Virtual storage is applied to the peak shaving of a distribution network in the Turin DH system. Results show that the virtual storage leads to a reduction of about 25% of the morning thermal peak. This is a very encouraging results and it gives reasons to continue the virtual storage research for thermal peak shaving.

Nomenclature

$T1$	primary side supply temperature, K
$T2$	primary side return temperature, K
$\dot{m}_h$	primary side flow, kg/s
$T3$	secondary side supply temperature, K
$T4$	secondary side return temperature, K
$\dot{m}_c$	secondary side flow, kg/s
$T5$	heating device outlet temperature, K
T_{house}	average building temperature, K
V	building volume, m^3
ϕ_I	heat flux of heat exchanger between primary and secondary side, W
ϕ_h	heat flux required by the building, W
ϕ_{loss}	thermal losses of the building, W
k	global heat transfer coefficient, $W/(m^3K)$
c	thermal capacity of the building, $J/(m^3K)$
Δt_{delay}	pipe running delay, s

References

[1] Lund, H., Möller, B., Mathiesen, B. V., & Dyrelund, A. (2010). The role of district heating in future renewable energy systems. *Energy*, 35(3), 1381-1390.

[2] Rezaie, B., & Rosen, M. A. (2012). District heating and cooling: Review of technology and potential enhancements. *Applied Energy*, 93, 2-10.

[3] Self, S. J., Reddy, B. V., & Rosen, M. A. (2013). Geothermal heat pump systems: Status review and comparison with other heating options. *Applied Energy*, *101*, 341-348.

[4] Bi, Y., Guo, T., Zhang, L., & Chen, L. (2004). Solar and ground source heat-pump system. *Applied Energy*, *78*(2), 231-245.

[5] Sciacovelli, A., Guelpa, E., & Verda, V. (2014). Multi-scale modeling of the environmental impact and energy performance of open-loop groundwater heat pumps in urban areas. *Applied Thermal Engineering*, *71*(2), 780-789.

[6] Dotzauer, E. (2002). Simple model for prediction of loads in district-heating systems. *Applied Energy*, *73*(3), 277-284.

[7] Werner, S. (1984). The heat load in district heating systems (Doctoral dissertation, Chalmers tekniska högskola).

[8] Nielsen, H. A., & Madsen, H. (2006). Modelling the heat consumption in district heating systems using a grey-box approach. *Energy and Buildings*, 38(1), 63-71.

[9] Guelpa, E., Toro, C., Sciacovelli, A., Melli, R., Sciubba, E., & Verda, V. (2016). Optimal operation of large district heating networks through fast fluid-dynamic simulation. *Energy*, 102, 586-595.

[10] Gadd, H., & Werner, S. (2013). Heat load patterns in district heating substations. *Applied energy*, 108, 176-183.

[11] Gadd, H., & Werner, S. (2014). Achieving low return temperatures from district heating substations. *Applied Energy*, 136, 59-67.

[12] Verda, V Guelpa E. (2016). Thermal peak load shaving through users request variations. *International Journal of Thermodynamics*, 19(3), 168-176.

[13] Guelpa, E., Barbero, G., Sciacovelli, A., & Verda, V. (2017). Peak-shaving in district heating systems through optimal management of the thermal request of buildings. *Energy*, *137*, 706-714.

[14] Brundu, F. G., Patti, E., Osello, A., Del Giudice, M., Rapetti, N., Krylovskiy, A., ... & Acquaviva, A. (2017). IoT Software Infrastructure for Energy Management and Simulation in Smart Cities. *IEEE Transactions on Industrial Informatics*, 13(2), 832-840.

[15] F. Orecchini, V.Naso., Energy Systems in the Era of Energy Vectors. Springer 2011]

[16] F.P. Incropera, D.P. DeWitt, Fundamentals of Heat and Mass Transfer, 3rd edition. Wiley, New York 1990

[17] F. Harary, Graph Theory, New Delhi: Narosa Publishing House ,1995.

[18] A. Sciacovelli, V. Verda, R. Borchiellini, Numerical Design of Thermal Systems, Torino: Clut, 2015

[19] Elisa, G., Sciacovelli A., & Vittorio, V. (2017). Thermo-fluid dynamic model of large district heating networks for the analysis of primary energy savings. *Energy*.